Bistable multipole quantum droplets in binary Bose-Einstein condensates

Liangwei Dong ⓘ,[1,2,*] Dongshuai Liu,[1] Zhijing Du,[1] Kai Shi,[1] and Wei Qi[1,2]

[1]*Department of Physics, Shaanxi University of Science & Technology, Xi'an 710021, China*
[2]*Institute of Theoretical Physics, Shaanxi University of Science & Technology, Xi'an 710021, China*

We address the existence and stability of multipole quantum droplets in symmetric binary Bose-Einstein condensates described by the amended Gross-Pitaevskii equation with Lee-Huang-Yang quantum corrections. Quantum droplets trapped in a weakly anharmonic potential can be composed of different numbers of globally linked poles with an azimuthally periodic distribution. Due to the competing Lee-Huang-Yang-augmented nonlinearity, the norm of two branches of droplets with slopes of opposite sign merges together at a lower cutoff of chemical potential. The lower and upper branches of droplets at the same chemical potential, but with a different norm, can evolve stably in certain parameter regions simultaneously. The stability domain of droplets shrinks with the growth of the number of poles. Even unstable necklacelike droplets can survive for a very long time.

I. INTRODUCTION

The last few years have witnessed rapid advances in the evolution dynamics of quantum droplets (QDs) [1–6]. In a pioneering work [1], the existence of stable solitonlike liquid states was predicted in binary Bose-Einstein condensates (BECs), where the intercomponent attraction was made slightly stronger than the intracomponent repulsion. Using the conventional Bogoliubov theory [7] with a modification, Petrov showed that the mechanical collapse anticipated from the mean-field approximation can be stabilized by the first-order Lee-Huang-Yang (LHY) correction due to quantum fluctuations [8].

In 2018, quasi-two-dimensional (2D) QDs (strongly compressed in one direction) [5,9], and three-dimensional (3D) isotropic QDs [10] were observed in mixtures of two different atomic states in ^{39}K and in an attractive mixture of ^{41}K and ^{87}Rb atoms [11] with contact interactions. QDs are nearly incompressible liquids self-sustained by competing nonlinearities: a cubic mean-field attraction and LHY-induced quartic repulsion characterized by the *s*-wave scattering lengths $a_{11} > 0$, $a_{22} > 0$, and $a_{12} < 0$, respectively. QDs are more than two orders of magnitude larger and eight orders of magnitude more dilute than liquid helium [3–6], and thus constitute the most dilute liquid in the world. Ultradilute droplets have found promising applications in matter-wave interferometry [12] and manipulations of quantum information [13].

Besides binary BECs, QDs also form in other systems with competing interactions. Particularly, when the attractive dipolar interaction is partially counterbalanced by the repulsive magnetic interaction occurring on top of the usual zero-range interactions, such as the ones taking place in potassium [3,14–17], anisotropic and longer-lived liquid states can form.

Supersolidlike QDs were demonstrated in dipolar condensates [18–23]. Droplets were also investigated in binary dipolar BECs [24,25].

Many numerical studies based on LHY-amended Gross-Pitaevskii equations (GPEs) [1,2,26–37] and the diffusion Monte Carlo technique [38–40] were performed on QDs in various dimensions. Theoretically, the QDs in full many-body systems solved by quantum Monte Carlo methods are in reasonable agreement with the predictions of the LHY-GPE framework, both for Bose-Bose mixtures and dipolar quantum gases [40–43].

Ring-shaped clusters constructed from several identical QDs are very robust [27]. Stable 2D vortex droplets with a topological charge up to 5 can be found provided that their norm exceeds a critical value [28]. Yet, stable 3D vortex droplets are possible only for vortices with charge up to 2 [29]. Stable QDs with a heterosymmetric or heteromultipole structure were also revealed [30].

QDs in an external potential also exhibit rich evolution dynamics. On-site- and intersite-centered semidiscrete fundamental and vortex droplets can be trapped stably in a nearly 1D array [31]. Robust rotating vortex clusters were revealed in binary BECs loaded in a combined harmonic-Gaussian potential [32]. Monopole oscillations of LHY fluid were observed in a ^{39}K spin mixture confined in a spherical trap potential [33]. Optical lattices significantly alter the existence and stability domain of QDs, either in one [34,35] or two dimensions [36]. Very recently, we predicted a different type of 2D and 3D stable QDs persistently rotating in an anharmonic potential. Through rotation, crescentlike droplets bridge the fundamental and vortex droplets with different topological charges [37].

The LHY correction can be used to stabilize not only fundamental states, but also excited states. Thus far, in 2D and 3D configurations, stable excited QDs were found only in the form of vortex states [28,29]. Therefore, a fascinating question arises about whether other families of higher-order

QDs, e.g., multipole-mode droplets, exist. If yes, what is their dynamics and how does the LHY correction influence their dynamics? Note that various types of multipole nonlinear states have been considered in different configurations [44–47], but not, as yet, for QDs.

In this paper, we show that multipole QDs can form out of a gaseous binary BEC described by the amended GPE. The aim of this paper is twofold. First, we reveal that two branches of azimuthally periodic droplets including different numbers of poles exist in symmetric binary BECs. Second, we investigate the stability of multipole QDs and find the shrinkage of the stability domain with the growth of the number of poles. Unstable necklacelike droplets survive for a long time.

II. THEORETICAL MODEL

Since the form of the LHY correction changes upon reduction of the dimensionality, the properties of QDs depend on the dimensionality of the LHY system [1,2]. The evolution dynamics of 3D binary BEC can be described by the GPE equation with a self-attractive cubic term augmented with LHY-induced quartic self-repulsion [1]. When BEC is strongly confined in the transverse direction, the reduced 2D LHY system significantly simplifies the descriptions of binary BEC for modes with lateral size $l \gg \sqrt{a_\pm a_\perp}$, where $a_\pm$ and $a_\perp$ denote the self-repulsion scattering lengths of each component and the transverse-confinement length, respectively [48]. For typical values used in experiments $l \sim 10 \ \mu m$, $a_\pm \sim 3$ nm, and $a_\perp \leqslant 1 \ \mu m$, the above condition results in reduced coupled GPEs [1,2] for describing the evolution of a two-component binary BEC with dimensionless wave functions $\Psi_\pm(x, y, t)$,

$$i\frac{\partial \Psi_\pm}{\partial t} = -\frac{1}{2}\nabla^2 \Psi_\pm + V\Psi_\pm + \frac{4\pi}{g}(|\Psi_\pm|^2 - |\Psi_\mp|^2)\Psi_\pm$$
$$+ (|\Psi_+|^2 + |\Psi_-|^2)\ln(|\Psi_+|^2 + |\Psi_-|^2)\Psi_\pm. \quad (1)$$

Here, $\nabla^2 = \partial_{xx} + \partial_{yy}$ is the transverse Laplace operator. The coordinates and time are additionally rescaled by the relations $(x, y) \rightarrow (g/2\sqrt{\pi})(x, y)$ and $t \rightarrow (g^2/4\pi)t$ with $g > 0$ being a coupling constant. For the sake of simplicity, we assume identical shapes of the components, i.e., $a_+ = a_-$ and $\Psi_+ = \Psi_- = \psi/\sqrt{2}$. The identical intraspecies interactions thus allow one to reduce the full binary system to a scalar equation with an external potential,

$$i\frac{\partial \psi}{\partial t} = -\frac{1}{2}\nabla^2 \psi + |\psi|^2 \ln(|\psi|^2)\psi + V\psi. \quad (2)$$

This system conserves several quantities, including the norm (number of atoms) $N = \iint |\psi|^2 dx dy$ and the Hamiltonian (energy),

$$E = \frac{1}{2}\iint \left[|\nabla\psi|^2 + 2V|\psi|^2 + |\psi|^4 \ln\left(\frac{|\psi|^2}{\sqrt{e}}\right)\right]dx dy.$$

We consider the evolution of QDs in a weakly anharmonic potential $V = (-\alpha r^2 + \beta r^4)/2$, where $r = \sqrt{x^2 + y^2}$ and anharmonic parameters $\alpha = 10^{-2}$ and $\beta = 10^{-4}$, as in Ref. [37]. Such a potential provides a shallow radial minimum for trapping necklacelike droplets [Fig. 1(a)]. Stationary solutions of QDs can be solved numerically by assuming
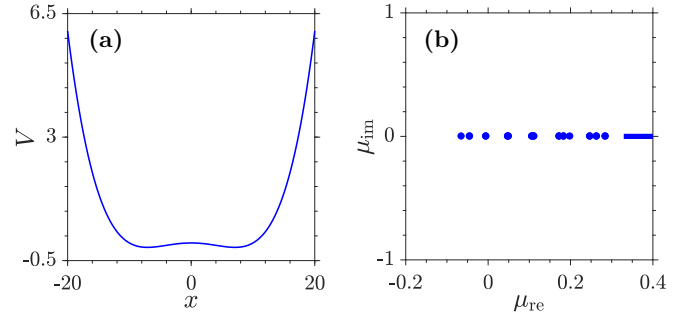

FIG. 1. (a) Potential V. (b) Spectra of a linear system. All quantities are plotted in dimensionless units

$\psi = w(x, y)\exp(-i\mu t)$. Substitution of it into Eq. (2) results in an ordinary differential equation,

$$\frac{1}{2}\nabla^2 w + \mu w - V w - |w|^2 \ln(|w|^2)w = 0, \quad (3)$$

where w denotes the distribution of stationary QDs at $t = 0$ and μ is the chemical potential of the condensate.

III. NUMERICAL RESULTS AND DISCUSSIONS

Before we discuss the properties of QDs in a nonlinear system, it is instructive to understand the dispersion relation of the corresponding linear system. After removing the nonlinear term in Eq. (3), the linear equation has infinite eigenvalues and corresponding linear eigenmodes. Nonlinear modes can bifurcate from these linear modes if nonlinearity cannot be ignored. Fundamental droplets always bifurcate from the first linear mode and higher-order excited droplets associate with other linear modes. Linear modes intuitively reveal the possible profiles of nonlinear modes bifurcating from them. The spectra of the given potential are shown in Fig. 1(b). The first five discrete μ values are $\mu_0 = -0.6481$, $\mu_1 = -0.0445$, $\mu_2 = -0.0049$, $\mu_3 = -0.0481$, and $\mu_4 = 0.1116$. At these μ values, QDs with topological charges $m = 0, 1, 2, 3$, and 4 can bifurcate out from the corresponding linear modes. Meanwhile, the bifurcation of droplets with 0, 2, 4, 6, and 8 poles from the linear modes is also possible, as we will show later.

The distributions of dipole QDs are shown in Fig. 2. Droplets composed of two well-separated spots shown in the upper panels originate from the linear mode at $\mu_1 = -0.0445$. They can be seen as the superposition states of two vortex droplets with opposite winding number $m = \pm 1$. Thus, the linear eigenvalue from which dipole droplets bifurcate out equals the linear eigenvalue where vortex droplets with $m = \pm 1$ bifurcate out. With the growth of μ, the droplet becomes broad and its amplitude decreases [Figs. 2(a) and 2(b)]. This family of droplets ceases to exist when $\mu < -0.3392$. In addition to droplets bifurcating from linear modes, there exists another family of droplets with a broader distribution of each pole. This family of droplets is composed of two half-moon components [Figs. 2(c) and 2(d)]. Their components expand with the growth of μ. Meanwhile, the amplitude of the droplet increases slowly.

While the norm of the lower-branch droplets increases monotonically with a decrease of μ, the norm of the upper-branch droplets increases with the growth of μ
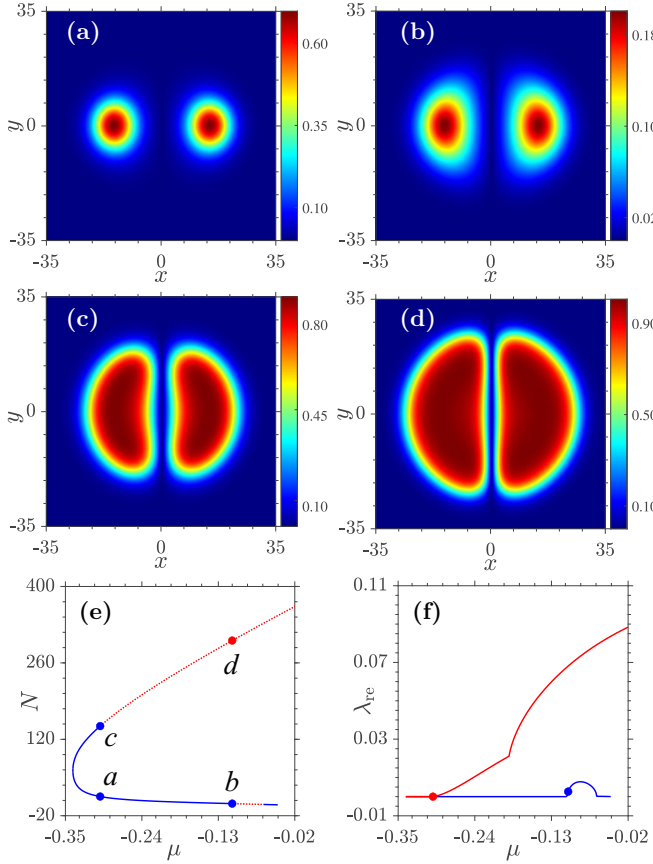
FIG. 2. Moduli of dipole droplets marked by circles in (e). $\mu = -0.30$ in (a), (c) and -0.11 in (b), (d). The color bars depict the dimensionless amplitudes of droplets here and afterwards. (e) Dependence of norm N on chemical potential μ. Dotted: unstable; solid: stable. (f) Instability growth rate $\lambda_{\rm re}$ vs μ for lower branch (blue) and upper branch (red) droplets. All quantities are plotted in dimensionless units.
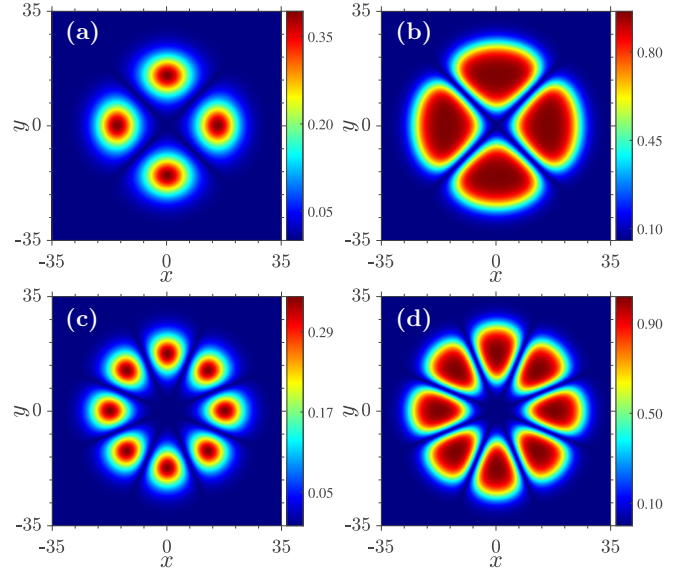

FIG. 3. (a), (b) Quadrupole and (c), (d) octupole droplets marked by circles in Fig. 4(a) at $\mu = -0.17$ and Fig. 4(b) at $\mu = -0.04$. (a), (c) Lower branch. (b), (d) Upper branch. All quantities are plotted in dimensionless units.

[Fig. 2(e)]. The rapid rise of the norm of the upper-branch droplets means that the number of atoms in the droplets increases rapidly with the growth of μ. Interestingly enough, the two branches of the droplets merge together at the common lower cutoff of the chemical potential $\mu_{\rm cut} = -0.3392$. The slope of the norm curve at $\mu_{\rm cut}$ is vertical.

The stability of the droplets is very important since it determines whether droplets can survive for a long time and thus is crucial to practical applications of them. The stability of the droplets can be analyzed by means of the linearized Bogoliubov–de Gennes equations [49,50] for perturbed wave functions, taken as

$$\psi(x, y, t) = [w + f \exp(\lambda t) + g^* \exp(\lambda^* t)] \exp(-i\mu t),$$

where $f(x, y), g(x, y) \ll 1$ are infinitesimal perturbations which may grow with a common complex growth rate λ of the disturbance upon evolution, and $*$ is the complex conjugate operation. The linearization of Eq. (1) for these perturbations yields a linear-stability eigenvalue problem

$$\lambda \begin{bmatrix} f \\ g \end{bmatrix} = i \begin{bmatrix} M_1 & M_2 \\ -M_2^* & -M_1^* \end{bmatrix} \begin{bmatrix} f \\ g \end{bmatrix}. \quad (4)$$

Here, $M_1 = -\frac{1}{2}\nabla^2 + V - \mu + 2|w|^2[\ln(|w|^2) + \frac{1}{2}]$ and $M_2 = w^2[\ln(|w|^2) + 1]$. Equations (4) can be solved numerically by the Fourier collocation algorithm put forward by Yang [51]. The stability of a QD is determined by the spectrum of the above linearization operator. Droplets can evolve stably only when all imaginary parts of eigenvalue λ equal zero.

The lower-branch dipole droplets are unstable in a narrow region near the linear bifurcation point $\mu_1 = -0.0445$. The upper-branch dipoles are stable in the scope $\mu \in [-0.3392, -0.2997]$. Near the lower cutoff of μ, there exists a common stability region where both the lower and upper branches of dipoles are stable. Borrowing the concept of bistable solitons in optics [52], we term these self-localized droplet states with the same μ but different norm N as "bistable" droplets. We also note that the stability of the lower and upper branches of the droplets supported by LHY-GPE does not obey the Vakhitov-Kolokolov stability criterion [53], which holds true usually for optical solitons or matter-wave solitons. Figure 2(f) displays the dependence of the instability growth rate on chemical potential μ.

Now, we address the properties of droplets with more components. The profiles of quadrupole and octupole droplets are shown in Fig. 3. Similar to dipole droplets, while the components of the lower-branch quadrupoles are well separated, the spots of droplets on the upper branch are broad [Figs. 3(a) and 3(b)]. This indicates that the interplay between the components of the upper-branch droplets is strong. Meanwhile, two neighboring components of an octupole droplet are a little closer than those for a quadrupole droplet [Figs. 3(a) and 3(c)]. The radius of a multipole mode droplet (the distance from the center of one component to the origin) slightly increases with the growth of the number of spots [Figs. 3(a) and 3(c)]. Due to the confinement of the external potential,
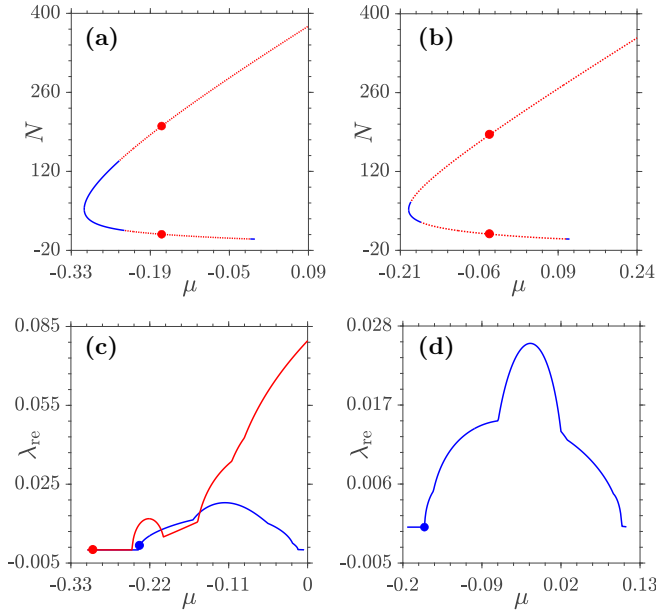
FIG. 4. Norm N vs μ for (a) quadrupole and (b) octupole droplets. Dotted: unstable; solid: stable. Instability growth rate vs μ for (c) quadrupole and (d) octupole droplets. The lower branch is shown in blue and the upper branch in red. All quantities are plotted in dimensionless units.

FIG. 5. (a), (b) Necklace droplets with 14 poles marked in (c) at $\mu = 0.27$. (c) Dependence of norm N of necklace droplets on μ. Dotted: unstable; solid: stable. Inset: Amplification of the region near μ_{cut}. (d) Instability growth rate vs μ for lower-branch droplets. All quantities are plotted in dimensionless units.

the components of octupole droplets on the upper branch are obviously squeezed on the azimuthal direction and expand along the radial direction [Fig. 3(d)].

The norm of the lower-branch quadrupole droplets originating from the linear mode at $\mu_2 = -0.0049$ merges with the norm curve of the upper-branch quadrupole droplets at $\mu_{\mathrm{cut}} = -0.3071$ [Fig. 4(a)]. The merging point for octupole droplets is $\mu_{\mathrm{cut}} = -0.1942$ [Fig. 4(b)]. The shift of μ_{cut} for droplets with different numbers of poles is merely due to the different linear eigenvalues of μ from which the lower-branch droplets bifurcate out. Though the norm curve of the upper-branch droplets can continue to even higher values for larger μ, we do not pay more attention to the corresponding multipole droplets since they are unstable.

Comparing Fig. 2(f) with 4(c), one finds that the stability domain of the lower-branch droplets shrinks rapidly with the growth of the number of droplet poles. The stability region of the upper-branch droplets shrinks at a relatively slow rate. Octupole droplets are stable in a very narrow region near their merging point of μ. Note that the stability of the multipole droplets trapped in a potential are very different from that of vortex droplets in the LHY system without an external potential [28,29], where vortices with different topological charges are stable only when the norm (number of atoms) exceeds a critical value.

To further understand the properties of multipole droplets, we investigate necklacelike droplets with 10, 12, and 14 components. Representative profiles of droplets including 14 poles are illustrated in Figs. 5(a) and 5(b). The lower-branch necklacelike droplets bifurcate from the linear mode at $\mu = 0.3499$. The merging point of μ for two branches of droplets now is shifted to 0.0428. Due to the repulsion between neigh-
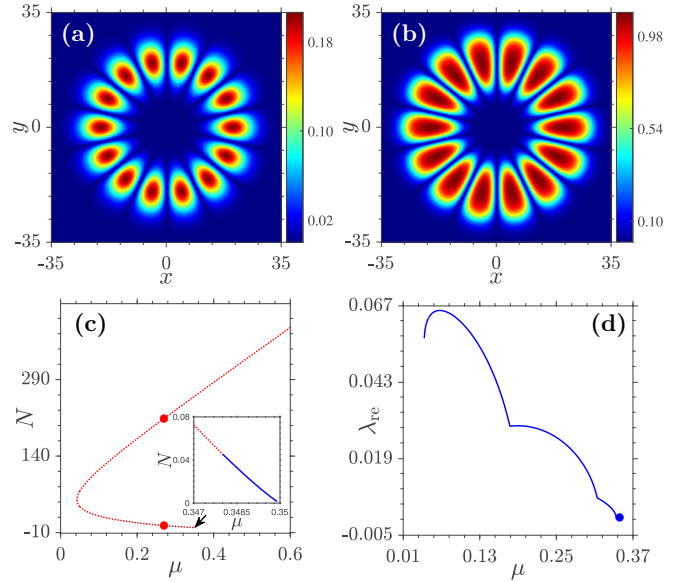
boring poles, the effective radius of droplets with more poles is larger than those with fewer poles. For the same reason, the poles of necklace droplets on the lower and upper branches are squeezed on the azimuthal direction and expand along the radial direction more obviously. The strong interactions between the neighboring poles are responsible for the instability of droplets with more poles [Fig. 5(c)]. The narrow stability region of octupole droplets near μ_{cut} disappears when the number of poles increases to 14. Such droplets are unstable in almost their whole existence domain [Fig. 5(d)].

To verify the stability analysis results of QDs with various numbers of poles, we perform extensive evolution simulations of droplets by the split-step Fourier method. In the numerical simulations, we add white noise into the initial input at $t = 0$ for stable droplets and do not add noise for unstable droplets. Typical evolution examples of stable and unstable droplets are shown in Fig. 6. The very small instability growth rates of unstable droplets shown in Figs. 2(f), 4(c), 4(d) and 5(d) imply that even unstable droplets can survive for a very long time [Figs. 6(a) and 6(d)]. One or more spots of unstable QDs decay with an increase of t and disappear eventually. The left spot corresponds to a symmetry-breaking state of the system. White noise added into the stable droplets radiates away quickly for a short time. Good agreements between the stability analysis and direct numerical evolution simulations are obtained for all addressed multipole mode droplets. Note the droplet shown in Fig. 6(f) is very close to the corresponding linear eigenmode.

We briefly explain the physics of the coexistence of two branches of droplets. When the condensate includes a few atoms, the atoms are confined in the low-lying area of the anharmonic potential shown in Fig. 1(a). Such droplets reside on the lower branch and bifurcate from the corresponding
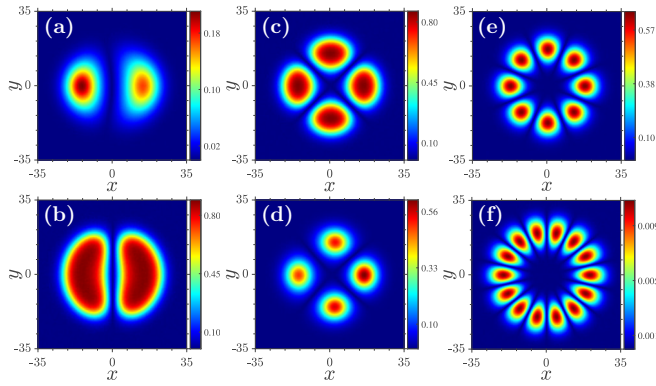
FIG. 6. Evolution simulations of (b), (c), (e), (f) stable and (a), (d) unstable QDs. (a) Unstable lower-branch dipole droplet marked in Fig. 2(f) at $\mu = -0.106$, $t = 2400$. (b) Stable upper-branch dipole droplet marked in Fig. 2(f) at $\mu = -0.3$, $t = 6000$. (c), (d) Stable upper-branch quadrupole droplets at $\mu = -0.299$, $t = 6000$ and unstable lower-branch quadrupole droplets at $\mu = -0.234$, $t = 3120$ marked in Fig. 4(c). (e) Stable octupole droplet marked in Fig. 4(d) at $\mu = -0.17$, $t = 6000$. (f) Stable necklace droplet marked in Fig. 5(d) at $\mu = 0.349$, $t = 6000$. All quantities are plotted in dimensionless units.

linear mode. With a decrease of the chemical potential, the number of atoms increases until $\mu = \mu_{cut}$, where atoms fully occupy the low-lying area of the potential. At this stage, the LHY correction exhibits an attractive nonlinearity. The norm curve of the lower-branch droplets is a decreasing function of μ. With a further increase of droplet density, repulsive nonlinearity becomes dominant. It leads to a positive slope of the norm curve. The atoms in the upper-branch droplets cross the bulge at the bottom of the anharmonic potential and occupy the region at a level exceeding the potential bulge.

We should note that the analysis and all presented results are valid only in the zero-temperature limit (the relevant experimental setting is $\simeq 150$ nK [54]). Droplets at finite temperatures were investigated by the Hartree-Fock-Bogoliubov-Popov theory. A thermal component forms a halo around the droplets [55]. The arrangement and stability of the multipole droplets we discussed will change when the temperature is nonzero.

The coordinates $(x, y, t) = (Xr_0^{-1}, Yr_0^{-1}, Tt_0^{-1})$ have been used for the derivation of dimensionless Eqs. (1) and (2),

where r_0 is the characteristic transverse scale. The characteristic energy $\epsilon_0 = \hbar^2/mr_0^2$ (m is the atomic mass) and time $t_0 = \hbar\epsilon_0^{-1}$. By assuming $r_0 = 0.5\ \mu$m, one gets energy and unit timescales of $\epsilon_0 \sim 6.9 \times 10^{-31}$ J and $t_0 \sim 0.15$ ms. These estimates are based on the atomic mass of ^{39}K from recent experiments [5,10].

Experimentally, we consider ^{39}K atoms tightly confined by a transversal anharmonic potential. The s-wave scattering lengths are assumed as $a_{\pm} = -50.0a_0$ and $a = 50.5a_0$ for the inter- and intraspecies interactions (a_0 is the Bohr radius), respectively. The parameters of the external potential V are $\alpha = m\omega^2 r_0^2/\epsilon_0$ and $\beta = \gamma m\omega^2 r_0^4/\epsilon_0 d^2$, where ω is the trapping frequency, $d = (\hbar/m\omega)^{1/2}$ is the oscillator length, and γ is the anharmonicity parameter. The number of atoms $\mathcal{N}$ in the condensate connects with the dimensionless norm N by $\mathcal{N} = (\epsilon_0 r_0^3/g)N$, where the coupling constant $g = 4\pi\hbar^2 a_{\pm}/m$. The estimate of the experimental parameters based on the above assumptions corresponds roughly to $\omega \sim 600$ Hz, $\mathcal{N} \sim 6 \times 10^3$, $d = 1.5\ \mu$m, and $\gamma = 0.3$, which are well within the reach of current experimental investigations.

IV. CONCLUSIONS

To summarize, we investigated the existence, stability, and evolution dynamics of QDs including various numbers of poles distributed uniformly on a ring. The combination of competing LHY nonlinearity and an anharmonic potential allows for the coexistence of two branches of QDs at the same chemical potential but with different numbers of atoms. With the growth of the pole number, the stability domain of the droplets shrinks. Unstable multipole droplets are very robust and can survive for a long time. Our findings can be easily generalized into optical solitons in competing cubic-quintic nonlinear media trapped in an anharmonic potential.

ACKNOWLEDGMENTS

[1] D. S. Petrov, Quantum Mechanical Stabilization of a Collapsing Bose-Bose Mixture, Phys. Rev. Lett. **115**, 155302 (2015).

[2] D. S. Petrov and G. E. Astrakharchik, Ultradilute Low-Dimensional Liquids, Phys. Rev. Lett. **117**, 100401 (2016).

[3] M. Schmitt, M. Wenzel, F. Böttcher, I. Ferrier-Barbut, and T. Pfau, Self-bound droplets of a dilute magnetic quantum liquid, Nature (London) **539**, 259 (2016).

[4] Y. V. Kartashov, V. V. Konotop, D. A. Zezyulin, and L. Torner, Bloch Oscillations in Optical and Zeeman Lattices in the Presence of Spin-Orbit Coupling, Phys. Rev. Lett. **117**, 215301 (2016).

[5] C. R. Cabrera, L. Tanzi, J. Sanz, N. Naylor, P. Thomas, P. Cheiney, and T. L., Quantum liquid droplets in a mixture of Bose-Einstein condensates, Science **359**, 301 (2018).

[6] I. Ferrier-Barbut, Ultradilute quantum droplets, Phys. Today **72**(4), 46 (2019).

[7] D. M. Larsen, Binary mixtures of dilute Bose gases with repulsive interactions at low temperature, Ann. Phys. (NY) **24**, 89 (1963).

[8] T. D. Lee, K. Huang, and C. N. Yang, Eigenvalues and eigenfunctions of a Bose system of hard spheres and its low-temperature properties, Phys. Rev. **106**, 1135 (1957).

[9] P. Cheiney, C. R. Cabrera, J. Sanz, B. Naylor, L. Tanzi, and L. Tarruell, Bright Soliton to Quantum Droplet Transition in a Mixture of Bose-Einstein Condensates, Phys. Rev. Lett. **120**, 135301 (2018).

[10] G. Semeghini, G. Ferioli, L. Masi, C. Mazzinghi, L. Wolswijk, F. Minardi, M. Modugno, G. Modugno, M. Inguscio, and M. Fattori, Self-Bound Quantum Droplets of Atomic Mixtures in Free Space, Phys. Rev. Lett. **120**, 235301 (2018).

[11] C. D'Errico, A. Burchianti, M. Prevedelli, L. Salasnich, F. Ancilotto, M. Modugno, F. Minardi, and C. Fort, Observation of quantum droplets in a heteronuclear bosonic mixture, Phys. Rev. Research **1**, 033155 (2019).

[12] G. D. McDonald, C. C. N. Kuhn, K. S. Hardman, S. Bennetts, P. J. Everitt, P. A. Altin, J. E. Debs, J. D. Close, and N. P. Robins, Bright Solitonic Matter-Wave Interferometer, Phys. Rev. Lett. **113**, 013002 (2014).

[13] R. K. Bullough and M. Wadati, Optical solitons and quantum solitons, J. Opt. B: Quantum Semiclassical Opt. **6**, S205 (2004).

[14] B. Laburthe-Tolra, A strange kind of liquid, Nature (London) **539**, 176 (2016).

[15] I. Ferrier-Barbut, H. Kadau, M. Schmitt, M. Wenzel, and T. Pfau, Observation of Quantum Droplets in a Strongly Dipolar Bose Gas, Phys. Rev. Lett. **116**, 215301 (2016).

[16] I. Ferrier-Barbut, M. Wenzel, F. Böttcher, T. Langen, M. Isoard, S. Stringari, and T. Pfau, Scissors Mode of Dipolar Quantum Droplets of Dysprosium Atoms, Phys. Rev. Lett. **120**, 160402 (2018).

[17] L. Chomaz, S. Baier, D. Petter, M. J. Mark, F. Wächtler, L. Santos, and F. Ferlaino, Quantum-Fluctuation-Driven Crossover from a Dilute Bose-Einstein Condensate to a Macro-droplet in a Dipolar Quantum Fluid, Phys. Rev. X **6**, 041039 (2016).

[18] L. Tanzi, S. Roccuzzo, E. Lucioni, F. Famà, A. Fioretti, C. Gabbanini, G. Modugno, A. Recati, and S. Stringari, Supersolid symmetry breaking from compressional oscillations in a dipolar quantum gas, Nature (London) **574**, 382 (2019).

[19] M. Guo, F. Böttcher, J. Hertkorn, J.-N. Schmidt, M. Wenzel, H. P. Büchler, T. Langen, and T. Pfau, The low-energy Goldstone mode in a trapped dipolar supersolid, Nature (London) **574**, 386 (2019).

[20] L. Tanzi, E. Lucioni, F. Famà, J. Catani, A. Fioretti, C. Gabbanini, R. N. Bisset, L. Santos, and G. Modugno, Observation of a Dipolar Quantum Gas with Metastable Supersolid Properties, Phys. Rev. Lett. **122**, 130405 (2019).

[21] G. Natale, R. M. W. van Bijnen, A. Patscheider, D. Petter, M. J. Mark, L. Chomaz, and F. Ferlaino, Excitation Spectrum of a Trapped Dipolar Supersolid and Its Experimental Evidence, Phys. Rev. Lett. **123**, 050402 (2019).

[22] F. Böttcher, J.-N. Schmidt, M. Wenzel, J. Hertkorn, M. Guo, T. Langen, and T. Pfau, Transient Supersolid Properties in an Array of Dipolar Quantum Droplets, Phys. Rev. X **9**, 011051 (2019).

[23] F. Böttcher, J.-N. Schmidt, J. Hertkorn, K. S. H. Ng, S. D. Graham, M. Guo, T. Langen, and T. Pfau, New states of matter with fine-tuned interactions: Quantum droplets and dipolar supersolids, Rep. Prog. Phys. **84**, 012403 (2021).

[24] R. N. Bisset, L. A. P. n. Ardila, and L. Santos, Quantum Droplets of Dipolar Mixtures, Phys. Rev. Lett. **126**, 025301 (2021).

[25] J. C. Smith, D. Baillie, and P. B. Blakie, Quantum Droplet States of a Binary Magnetic Gas, Phys. Rev. Lett. **126**, 025302 (2021).

[26] G. E. Astrakharchik and B. A. Malomed, Dynamics of one-dimensional quantum droplets, Phys. Rev. A **98**, 013631 (2018).

[27] Y. V. Kartashov, B. A. Malomed, and L. Torner, Metastability of Quantum Droplet Clusters, Phys. Rev. Lett. **122**, 193902 (2019).

[28] Y. Li, Z. Chen, Z. Luo, C. Huang, H. Tan, W. Pang, and B. A. Malomed, Two-dimensional vortex quantum droplets, Phys. Rev. A **98**, 063602 (2018).

[29] Y. V. Kartashov, B. A. Malomed, L. Tarruell, and L. Torner, Three-dimensional droplets of swirling superfluids, Phys. Rev. A **98**, 013612 (2018).

[30] Y. V. Kartashov, B. A. Malomed, and L. Torner, Structured heterosymmetric quantum droplets, Phys. Rev. Research **2**, 033522 (2020).

[31] X. Zhang, X. Xu, Y. Zheng, Z. Chen, B. Liu, C. Huang, B. A. Malomed, and Y. Li, Semidiscrete Quantum Droplets and Vortices, Phys. Rev. Lett. **123**, 133901 (2019).

[32] M. N. Tengstrand, P. Stürmer, E. O. Karabulut, and S. M. Reimann, Rotating Binary Bose-Einstein Condensates and Vortex Clusters in Quantum Droplets, Phys. Rev. Lett. **123**, 160405 (2019).

[33] T. G. Skov, M. G. Skou, N. B. Jørgensen, and J. J. Arlt, Observation of a Lee-Huang-Yang Fluid, Phys. Rev. Lett. **126**, 230404 (2021).

[34] L. Dong, W. Qi, P. Peng, L. Wang, H. Zhou, and C. Huang, Multi-stable quantum droplets in optical lattices, Nonlinear Dyn. **102**, 303 (2020).

[35] Z. Zhou, X. Yu, Y. Zou, and H. Zhong, Dynamics of quantum droplets in a one-dimensional optical lattice, Commun. Nonlinear Sci. Numer. Simulat. **78**, 104881 (2019).

[36] Y.-Y. Zheng, S.-T. Chen, Z.-P. Huang, S.-X. Dai, B. Liu, Y.-Y. Li, and S.-R. Wang, Quantum droplets in two-dimensional optical lattices, Front. Phys. **16**, 22501 (2021).

[37] L. Dong and Y. V. Kartashov, Rotating Multidimensional Quantum Droplets, Phys. Rev. Lett. **126**, 244101 (2021).

[38] V. Cikojević, L. V. c. v. Markić, G. E. Astrakharchik, and J. Boronat, Universality in ultradilute liquid Bose-Bose mixtures, Phys. Rev. A **99**, 023618 (2019).

[39] V. Cikojević, L. V. Markić, and J. Boronat, Finite-range effects in ultradilute quantum drops, New J. Phys. **22**, 053045 (2020).

[40] L. Parisi, G. E. Astrakharchik, and S. Giorgini, Liquid State of One-Dimensional Bose Mixtures: A Quantum Monte Carlo Study, Phys. Rev. Lett. **122**, 105302 (2019).

[41] F. Cinti, A. Cappellaro, L. Salasnich, and T. Macrì, Superfluid Filaments of Dipolar Bosons in Free Space, Phys. Rev. Lett. **119**, 215302 (2017).

[42] A. Macia, J. Sánchez-Baena, J. Boronat, and F. Mazzanti, Droplets of Trapped Quantum Dipolar Bosons, Phys. Rev. Lett. **117**, 205301 (2016).

[43] V. Cikojević, K. Dželalija, P. Stipanović, L. Vranješ Markić, and J. Boronat, Ultradilute quantum liquid drops, Phys. Rev. B **97**, 140502(R) (2018).

[44] C. Rotschild, M. Segev, Z. Xu, Y. V. Kartashov, L. Torner, and O. Cohen, Two-dimensional multipole solitons in nonlocal nonlinear media, Opt. Lett. **31**, 3312 (2006).

[45] Y. V. Kartashov and L. Torner, Multipole-mode surface solitons, Opt. Lett. **31**, 2172 (2006).

[46] V. M. Lashkin, Two-dimensional nonlocal vortices, multipole solitons, and rotating multisolitons in dipolar Bose-Einstein condensates, Phys. Rev. A **75**, 043607 (2007).

[47] V. E. Lobanov, Y. V. Kartashov, and V. V. Konotop, Fundamental, Multipole, and Half-Vortex Gap Solitons in Spin-Orbit Coupled Bose-Einstein Condensates, Phys. Rev. Lett. **112**, 180403 (2014).

[48] Y. Li, Z. Luo, Y. Liu, Z. Chen, C. Huang, S. Fu, H. Tan, and B. A. Malomed, Two-dimensional solitons and quantum droplets supported by competing self- and cross-interactions in spin-orbit-coupled condensates, New J. Phys. **19**, 113043 (2017).

[49] L. P. Pitaevskii and S. Stringari, *Bose-Einstein Condensation* (Oxford University Press, Oxford, U.K., 2003).

[50] C. J. Pethick and H. Smith, *Bose-Einstein Condensation in Dilute Gases* (Cambridge University Press, Cambridge, U.K., 2008).

[51] J. Yang, *Nonlinear Waves in Integrable and Nonintegrable Systems* (SIAM, Philadelphia, 2010).

[52] A. E. Kaplan, Bistable Solitons, Phys. Rev. Lett. **55**, 1291 (1985).

[53] N. G. Vakhitov and A. A. Kolokolov, Stationary solutions of the wave equation in the medium with nonlinearity saturation, Radiophys. Quantum Electron. (Engl. Transl.) **16**, 783 (1973).

[54] G. Modugno, G. Ferrari, G. Roati, R. J. Brecha, A. Simoni, M. Inguscio, Bose-Einstein condensation of potassium atoms by sympathetic cooling, Science **294**, 1320 (2001).

[55] A. Boudjemâa, Quantum dilute droplets of dipolar bosons at finite temperature, Ann. Phys. **381**, 68 (2017).